

Electronic Supplementary Information

Triptycene-supported bimetallic salen porous organic polymers for high efficiency CO₂ fixation to cyclic carbonates

Yingting Zheng,^a Xiqian Wang,^a Chao Liu,^a Baoqiu Yu,^a Wenliang Li,^b Hailong Wang,^{*a}
Tingting Sun,^{*a} and Jianzhuang Jiang^{*a}

^a Beijing Advanced Innovation Center for Materials Genome Engineering, Beijing Key Laboratory for Science and Application of Functional Molecular and Crystalline Materials, Department of Chemistry, School of Chemistry and Biological Engineering, University of Science and Technology Beijing, Beijing 100083, China

^b Faculty of Chemistry, Northeast Normal University, Changchun 130024, China

* Corresponding author. E-mail: hlwang@ustb.edu.cn (H. Wang), ttsun99@ustb.edu.cn (T. Sun) and jianzhuang@ustb.edu.cn (J. Jiang)

Experimental section

General directions

All chemicals were employed as received without further purification. The bimetallic salen macrocycles (salen-Ni and salen-Co) were synthesized as reference according to the reported literature.^{S1}

Synthesis of BSPOPs

A mixture of 2,3,6,7,14,15-hexaammoniumtriptycene hexachloride (0.02 mmol, 13.8 mg), 2,6-diformyl-4-methylphenol (0.06 mmol, 9.8 mg), and metal salt (0.06 mmol, AlCl₃ 8.0 mg, Co(OAc)₂ 10.6 mg or Ni(OAc)₂ 10.6 mg) in 2.0 mL of mesitylene/EtOH (1:1 v/v) in a small vial was sonicated for 15 min. After adding the 180 μL ethanol solution of acetic acid (6.0 mol/L), the mixture was sonicated to afford a homogeneous dispersion. Then this solution was transferred into a pyrex tube and degassed by three freeze-pump-thaw cycles. The tube was sealed off and heated at 120°C for 72 h. The solid was collected by centrifugation and washed with anhydrous THF (3 × 6.0 mL) and acetone (3 × 6.0 mL). The powder was dried at 60°C under vacuum to afford the BSPOP-M (M = Al(III), Co(II), and Ni(II)). With respect to the synthesis of BSPOP-2H for the purpose of characterizing this series of POPs, the whole procedure is strictly followed the above mentioned one for the synthesis of BSPOP-M except without addition of metal salt. BSPOP-M (M = Al(III), Co(II), Ni(II), and BSPOP-2H) were obtained with the yield of 48%, 52%, 54% and 61%, respectively.

General procedure for CO₂ fixation to cyclic carbonates

Epoxide (15.0 mmol), metallic BSPOPs as catalyst (0.03 mmol, calculated based on

metal sites), and tetrabutylammonium bromide (TBAB) as co-catalyst (0.6 mmol) were added into a 25 mL reaction tube. The reaction mixture was stirred in the presence of carbon dioxide provided by a balloon at certain temperature. After a certain amount of time, the reaction was stopped. The catalysts were separated by centrifugation, and the resulting mixture was analyzed by ^1H NMR spectroscopy. For catalyst recycling measurement, the catalyst was separated from the reaction mixture by centrifugation and then rinsed with methanol, THF, and acetone, respectively. The recovered catalyst was dried and then reused in the next run. The recycling catalysis experimental was conducted under the above mentioned reaction conditions each time using the dry catalyst recycled from the last run.

Instrumentation

IR spectra were recorded as KBr pellets using a Bruker Tensor 37 spectrometer with 2.0 cm^{-1} resolution. Solid-state NMR spectra were collected on a 400 MHz Bruker Avance III spectrometer. Powder X-ray diffraction (PXRD) data were recorded on a TTR III multi-function X-ray diffractometer by depositing powder on a quartz sheet, from $2\theta = 2^\circ$ to 50° with 1° min^{-1} increments at room temperature. X-ray photoelectron spectra (XPS) data were collected from Thermo Scientific Escalab 250Xi photoelectron spectrometer. Scanning electron microscope (SEM) images and energy dispersive X-Ray spectroscopy (EDX) were obtained using a HITACHI SU8010 microscopy. The metal content determination was performed through analysis of the samples by inductively coupled plasma optical emission spectrometry (ICP-OES) on a Thermo IRIS Intrepid II XSP spectrometer. Thermal gravimetric analysis (TGA) data were collected on a LECO TGA701 analyzer with a heating rate of 5°C min^{-1} in the range of $25\sim 800^\circ\text{C}$ under N_2 atmosphere. The sorption isotherms were obtained using a Micromeritics ASAP 2020 PLUS HD88 surface area and porosity analyzer.

Before the gas sorption measurements, the powder samples of BSPOPs were degassed at 120°C for 12 h to drastically eliminate the volatile solvents blocked in pores. The permanent porosity of BSPOPs was examined with N₂ and CO₂ as adsorbate. The N₂ sorption isotherms were collected at 77 K, and CO₂ sorption isotherms were obtained at 196, 273, and 298 K, respectively. The temperature of 77, 196, 273, and 298 K was kept using liquid nitrogen bath, acetone/dry ice bath, ice water bath, and water bath at 25°C room with air-condition.

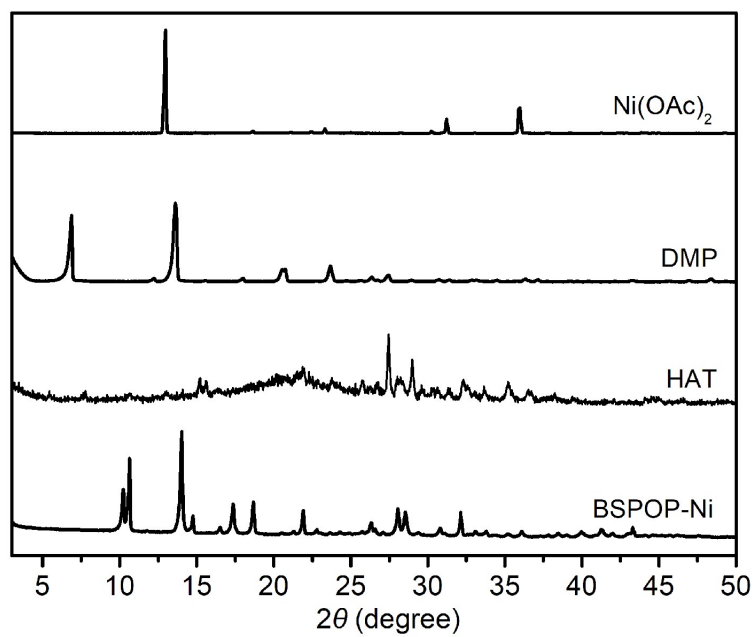


Fig. S1 Comparison of PXRD patterns between BSPOP-Ni, HAT, DMP and Ni(OAc)₂.

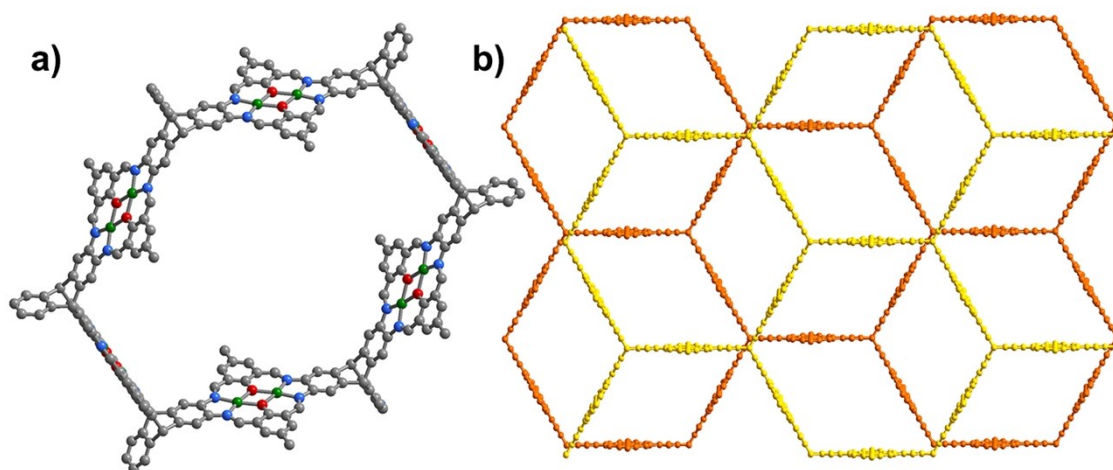


Fig. S2 A proposed structure model of BSPOP-Ni (a) macrocycle segment and (b) AB packing (different color representing different layers).

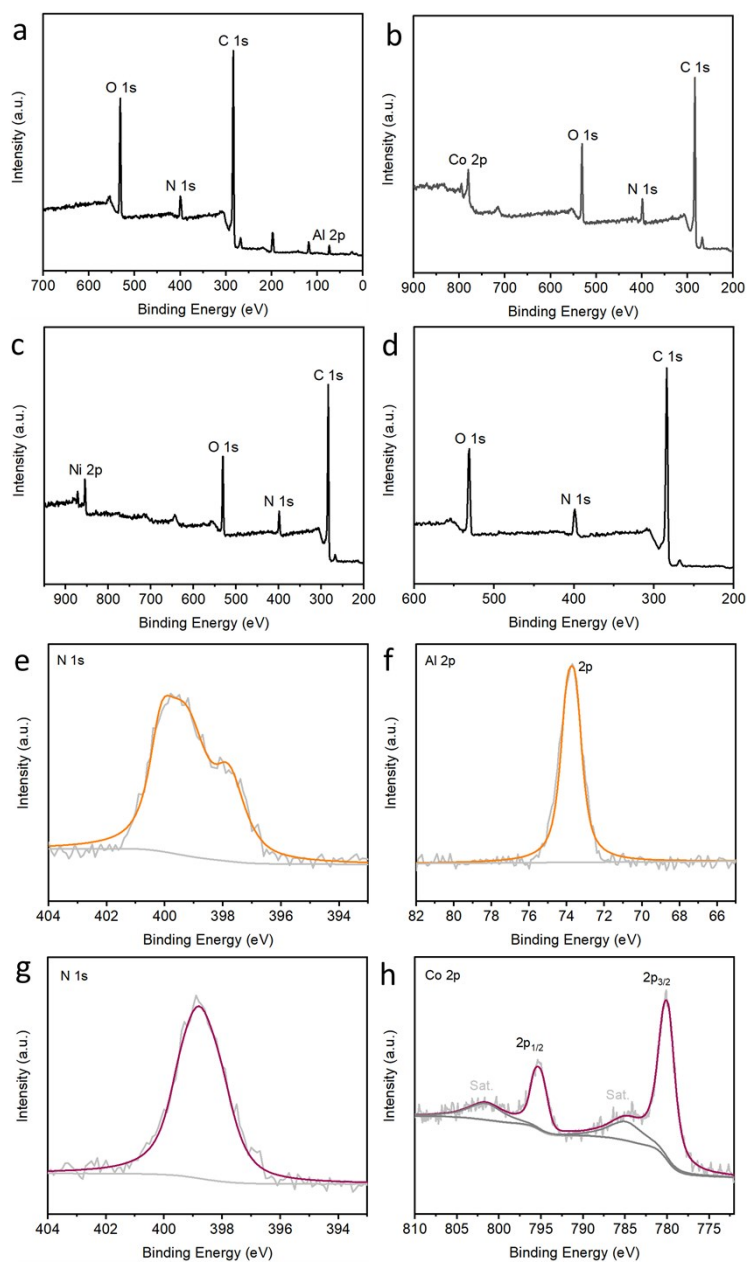


Fig. S3 XPS spectra of BSPOPs. (a) Survey scan of BSPOP-Al; (b) survey scan of BSPOP-Co; (c) survey scan of BSPOP-Ni; (d) survey scan of BSPOP-2H; (e) N 1s and (f) Al 2p of BSPOP-Al; (g) N 1s and (h) Co 2p of BSPOP-Co.

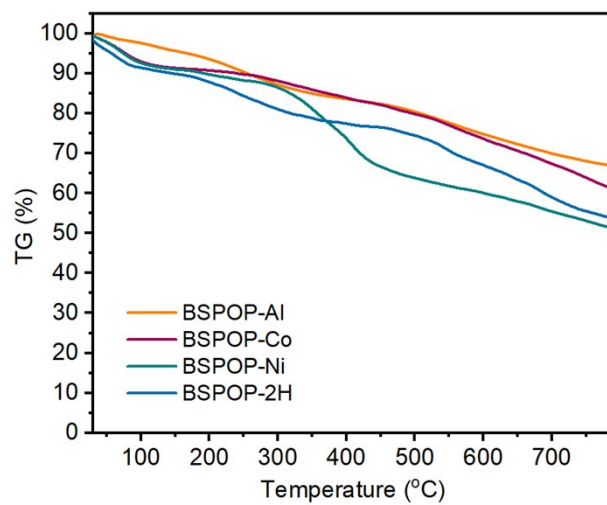


Fig. S4 Thermal gravimetric analysis (TGA) curves of BSPOPs.

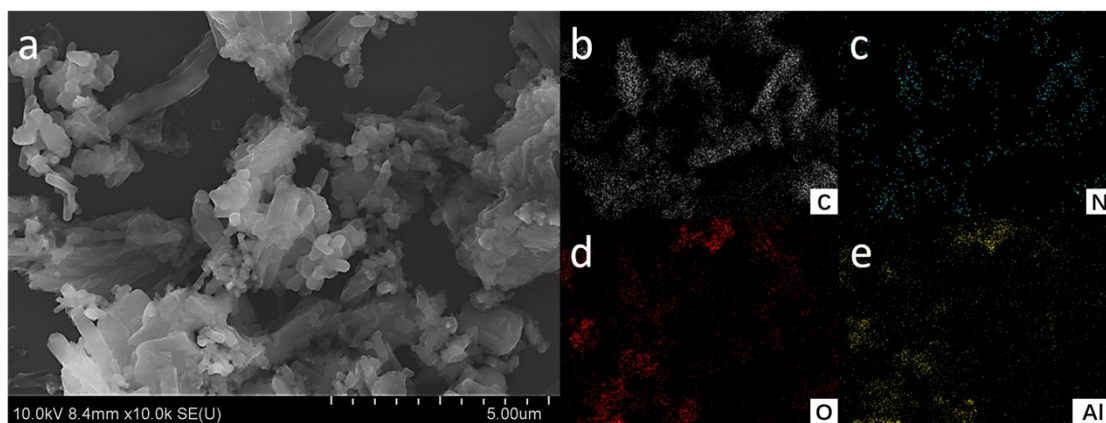


Fig. S5 (a) SEM and (b~e) EDX elemental mapping images of BSPOP-Al.

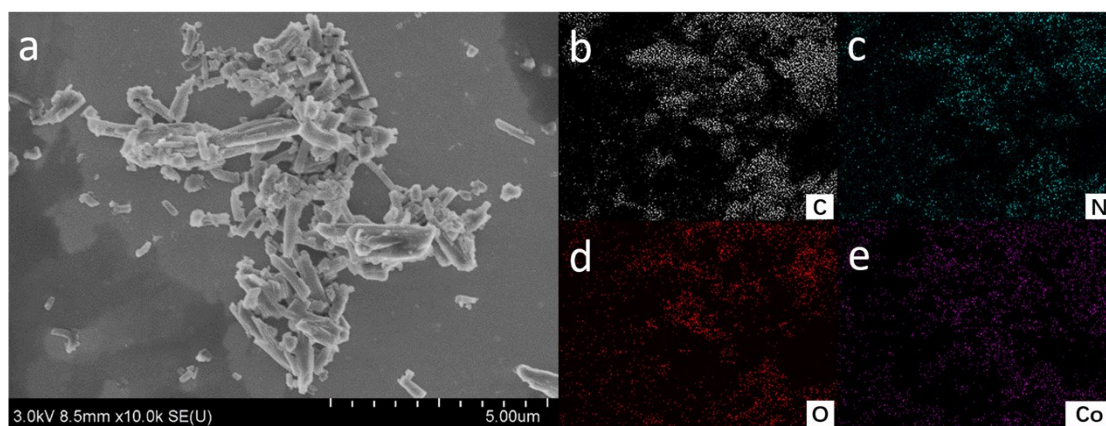


Fig. S6 (a) SEM and (b~e) EDX elemental mapping images of BSPOP-Co.

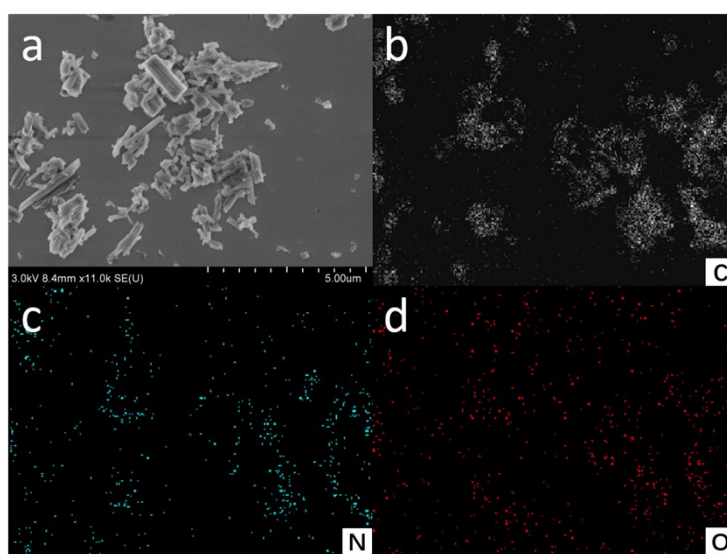


Fig. S7 (a) SEM and (b~d) EDX elemental mapping images of BSPOP-2H.

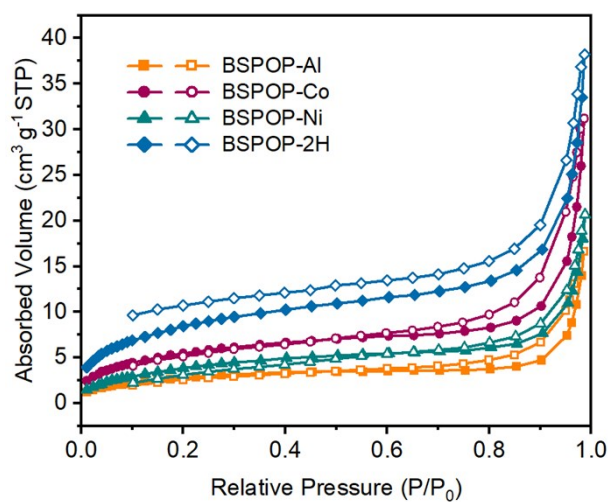


Fig. S8 Adsorption (filled) and desorption (empty) isotherms of N_2 at 77 K for BSPOPs.

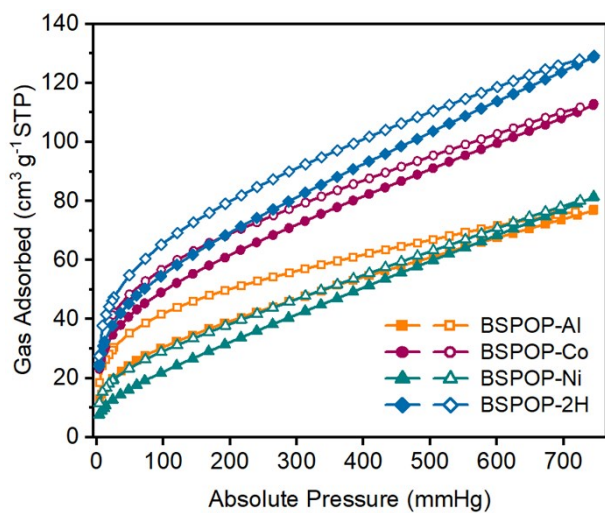


Fig. S9 Adsorption (filled) and desorption (empty) isotherms of CO_2 at 196 K for BSPOPs.

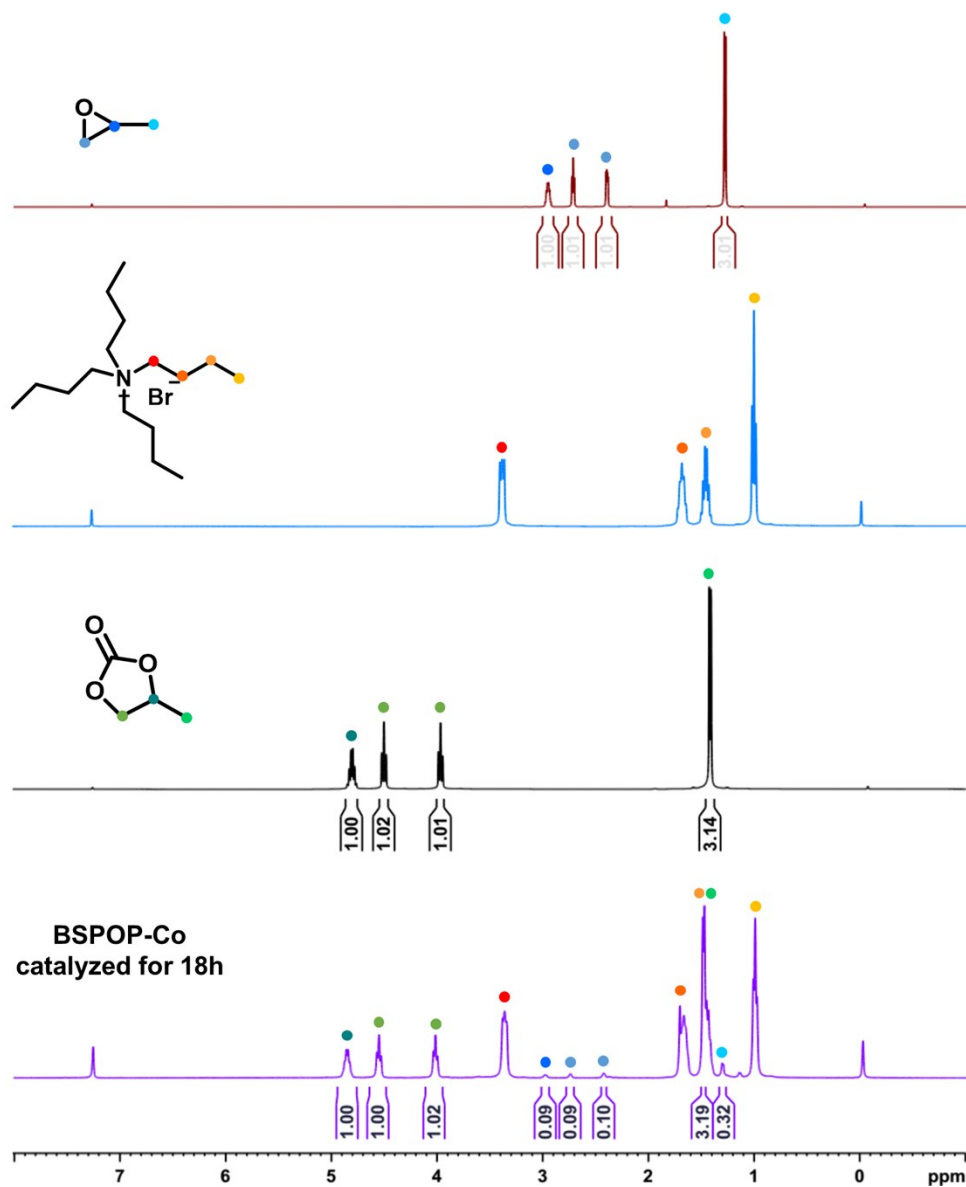


Fig. S10 ¹H NMR spectra of 1,2-epoxypropane, TBAB, propylene carbonate and BSPOP-Co catalyzed for 18h CO₂ cycloaddition reaction of 1,2-epoxypropane (from top to bottom). Un-marked peaks are for solvent.

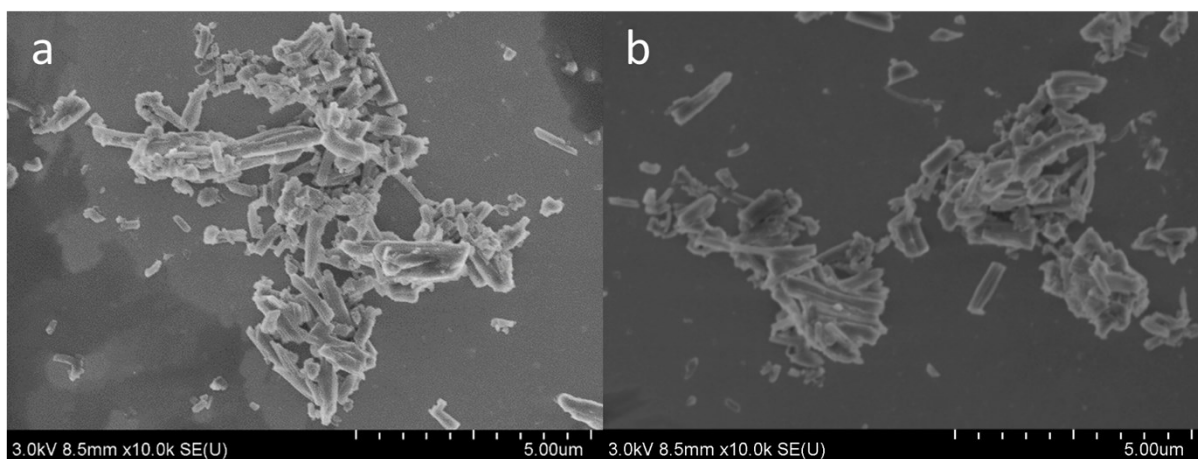


Fig. S11 SEM images of BSPOP-Co (a) before and (b) after catalysis for five runs.

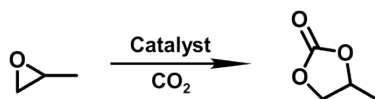
Table S1 The ICP-OES data of BSPOP-Al, BSPOP-Co and BSPOP-Ni

Sample	Analysis element	Theoretical value	Actual content
BSPOP-Al	Al	8.9%	8.8%
BSPOP-Co	Co	16.4%	15.0%
BSPOP-Ni	Ni	16.3%	16.9%

Table S2 CO₂ BET surface, adsorption and Q_{st} of BSPOPs

Sample	S_{BET}^a (m ² g ⁻¹)	CO ₂ absorbed volume (cm ³ g ⁻¹ STP) ^b		Q_{st}^c (kJ mol ⁻¹)
		273K	298K	
BSPOP-Al	160.4	19.4	13.9	26.5
BSPOP-Co	250.3	30.3	19.7	42.1
BSPOP-Ni	142.4	14.4	10.8	29.3
BSPOP-2H	280.5	31.8	22.4	30.0

^aBET surface area of BSPOPs. ^bCO₂ absorption at 760 mmHg. ^cIsosteric heat of CO₂ adsorption.

Table S3 Comparison of Catalytic Activity of Catalysts

Entry	Cat.	Temp.(°C)	Time(h)	p (atm)	Conv.(%)	TON	TOF(h ⁻¹)	Ref.
1	BSPOP-Co	25	18	1.0	92	460	26.6	This work
2	1-Co	22	48	1.0	26	130	3	S2
3	Co-CMP	25	48	1.0	81.5	167	3.5	S3
4	Co/POP-TPP	29	24	1.0	95.8	432	18	S4
5	POP-PBnCl-TPPMg-12	30	48	1.0	54.3	1086	22.6	S5
6	Al-CPOP	120	24	1.0	91	91	3.8	S6
7	DVB@ISA	60	24	10	99	396	16.5	S7
8	ZnPor-CP	80	16	10	32	400	25	S8

Table S4 The ICP-OES data of BSPOP-Co before and after catalysis

Sample	Analysis element	Theoretical value	Actual content
BSPOP-Co before catalysis	Co	16.4%	15.0%
BSPOP-Co after catalysis	Co	16.4%	12.8%

References

- S1 P. C. Swamy, E. Solel, O. Reany and E. Keinan, Synthetic Evolution of the Multifarene Cavity from Planar Predecessors, *Chem.-Eur. J.* **2018**, *24*, 15319–15328.
- S2 M. H. Alkordi, Ł. J. Weselinski, V. D'Elia, S. Barman, A. Cadiau, M. N. Hedhili, A. J. Cairns, R. G. AbdulHalim, J.-M. Basset and M. Eddaoudi, CO₂ Conversion: the Potential of Porous-Organic Polymers (POPs) for Catalytic CO₂-Epoxide Insertion, *J. Mater. Chem. A* **2016**, *4*, 7453–7460.
- S3 Y. Xie, T. T. Wang, X. H. Liu, K. Zou and W. Q. Deng, Capture and Conversion of CO₂ at Ambient Conditions by a Conjugated Microporous Polymer, *Nat. Commun.* **2013**, *4*, 1960–1966.
- S4 Z. Dai, Q. Sun, X. Liu, C. Bian, Q. Wu, S. Pan, L. Wang, X. Meng, F. Deng and F.-S. Xiao, Metalated Porous Porphyrin Polymers as Efficient Heterogeneous Catalysts for Cycloaddition of Epoxides with CO₂ under Ambient Conditions, *J. Catal.* **2016**, *338*, 202–209.
- S5 Z. Dai, Y. Tang, F. Zhang, Y. Xiong, S. Wang, Q. Sun, L. Wang, X. Meng, L. Zhao and F.-S. Xiao, Combination of Binary Active Sites into Heterogeneous Porous Polymer Catalysts for Efficient Transformation of CO₂ under Mild Condition, *Chinese J. Catal.* **2021**, *42*, 618–626.
- S6 T.-T. Liu, J. Liang, Y.-B. Huang and R. Cao, A Bifunctional Cationic Porous Organic Polymer Based on a Salen-(Al) Metalloligand for the Cycloaddition of Carbon Dioxide to Produce Cyclic Carbonates, *Chem. Commun.* **2016**, *52*, 13288–13291.
- S7 R. Luo, Y. Chen, Q. He, X. Lin, Q. Xu, X. He, W. Zhang, X. Zhou and H. Ji, Metallosalen-Based Ionic Porous Polymers as Bifunctional Catalysts for the Conversion of CO₂ into Valuable Chemicals, *ChemSusChem* **2017**, *10*, 1526–1533.
- S8 X. Liu, F. Zhou, M. Chen, W. Xu, H. Liu, J. Zhong and R. Luo, Synergistically Converting Carbon Dioxide into Cyclic Carbonates by Metalloporphyrin-Based Cationic Polymers with Imidazolium Functionality, *ChemistrySelect* **2021**, *6*, 583–588.